

## Shape Tuning of Type II CdTe-CdSe Colloidal Nanocrystal Heterostructures through Seeded Growth

Haizheng Zhong and Gregory D. Scholes\*

Department of Chemistry, 80 St. George Street, Institute for Optical Sciences, and Center for Quantum Information and Quantum Control, University of Toronto, Toronto, Ontario, M5S 3H6 Canada

Received May 7, 2009; E-mail: gscholes@chem.utoronto.ca

Colloidal semiconductor nanocrystal heterostructures (NHs) are formed by the epitaxial growth of a second material onto a preformed semiconductor nanocrystal. Depending on the relative energies of the valence and conduction orbitals of the two materials, the spectra and properties of NHs can be tuned dramatically compared to those of either material in isolation.<sup>1–3</sup> In type II core/shell NHs, the overlap between electron and hole wave functions, and thus the excitonic properties, is usually controlled by tuning the core diameter and shell thickness,<sup>4–6</sup> while shape effects of the NHs have been explored to a lesser extent.<sup>7–9</sup> Examples of type II NHs with anisotropic shapes have been reported, ranging from nanorods,<sup>7,8,10</sup> barbells,<sup>11</sup> tetrapods,<sup>7,12</sup> to multiple-branched rods.<sup>7,13</sup> In recent work we have found that shape-directed NHs provide excellent opportunities to study and control pathways and implications of electron–hole separation.<sup>8,9</sup> Here we report how striking shape variations can be achieved during CdTe-CdSe NH growth based solely on the size of the CdTe seed that forms the NH core.

Recent work has established the seeded growth method for tuning nanocrystal shape.<sup>14–17</sup> It has been shown that shape can be engineered between nanorods and tetrapods simply by tailoring the crystal phase of seeds. This method was successfully extended to synthesize type II ZnSe-CdS nanorods<sup>18,19</sup> and CdSe-CdTe tetrapods.<sup>20</sup> Here we show that type II CdTe-CdSe colloidal NHs in a variety of shapes, including an interesting Y-shaped structure, can be prepared reproducibly using the seeded growth method based on different sized seeds.

CdTe seeds were synthesized according to a modified published method.<sup>21</sup> Optical properties and transmission electron microscopy (TEM) observations indicated that the as-prepared CdTe seeds were of good quality, while powder X-ray diffraction (PXRD) showed that they had a zinc blend (ZB) phase (see Supporting Information (SI) Figures S1 and S2). CdTe-CdSe NHs were synthesized by growing CdSe on the preformed CdTe seeds through multiple-injection seeded growth. A fixed amount of CdTe seeds was mixed with a Cd precursor prepared by heating a mixture of octylphosphonic acid (OPA), tetradecylphosphonic acid (TDPA), trioctylphosphine oxide (TOPO), and CdO. The mixture was heated to a fixed temperature, and Se in trioctylphosphine (TOP) solution was added dropwise to the reaction system. A control experiment, without adding any seeds, was also conducted. The detailed synthetic procedures can be found in the SI.

Figure 1a shows the scanning transmission electron microscopy (STEM) images of the CdSe nanocrystals prepared in the control experiment where CdTe seeds were absent. CdSe nanorods, 5 nm wide and 70–80 nm long, were produced. Figure 1b–1f show STEM images of CdTe-CdSe NHs grown from CdTe seeds with average diameters of 2.6, 3.5, 4.3, 5.0, and 8.2 nm, respectively (overview images are shown in Supporting Information S3). We observed that the shape of the resulting CdTe-CdSe NHs was

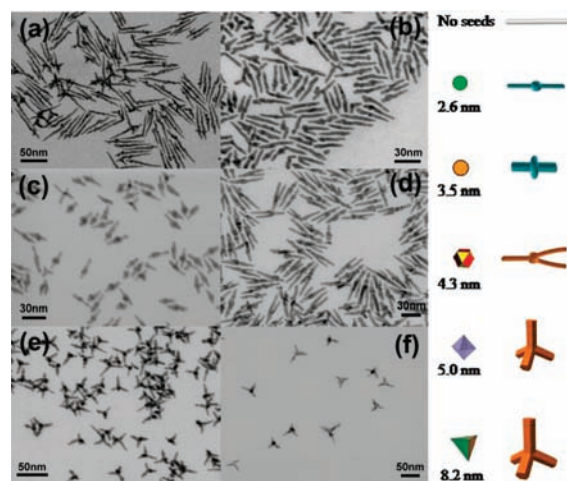


**Figure 1.** Left: (a) CdSe nanorods and (b–f) CdTe-CdSe NHs synthesized via epitaxial growth from CdTe seeds with average size of 2.6 (b), 3.5 (c), 4.3 (d), 5.0 (e), and 8.2 nm (f) respectively; Right: schematic diagram of the shape evolution of CdTe-CdSe NHs with seed size.

determined by the seed size: nanorods formed from 2.6 nm seeds, fat rods from 3.5 nm seeds, Y-shaped branched rods from 4.3 nm seeds, and tetrapods from both 5.0 and 8.2 nm seeds. The shape evolution is depicted schematically in the right part of Figure 1.

The NH shape appears to relate to the epitaxial growth on the seeds. One critical parameter influencing the growth pattern of NHs is the surface energy of crystallographic faces of the seeds.<sup>14,16</sup> We found that smaller CdTe seeds (<4 nm) tended to be nearly spherical, and they seeded bidirectional one-dimensional growth, producing CdTe-CdSe nanorods or fat rods. It was noted that larger seeds (>5 nm) have more obvious crystalline facets than smaller spherical ones. In this case, epitaxial CdSe growth was initiated on four (111) facets of the CdTe ZB phase, producing tetrapod heterostructures. The intermediate sized seeds (~4.3 nm) produced unique Y-shaped heterostructures. To our knowledge, this is the first observation of such Y-shaped nanocrystals. HRTEM analysis of a typical Y-shape NH, Figure 2, indicates that the Y-shaped NH has an asymmetric crystalline structure with a twinned ZB-CdTe seed at the center. At one end, a W-CdSe branch grew epitaxially along the <001> direction from the (111) plane of CdTe. At the other end, ZB-CdSe with many stacking faults grew on the two (111) planes of ZB-CdTe seeds and then changed phase to W-CdSe with one-dimensional growth in the <001> direction.

It has been observed that epitaxial growth from seeds is asymmetric.<sup>16,18,19</sup> This has been attributed to the reactivity difference between cation- and anion-rich ends. The (111) planes of ZB phase CdTe may terminate in Cd<sup>2+</sup>-rich facets or Te<sup>2-</sup>-rich facets.<sup>22</sup> The Cd<sup>2+</sup> end is capped by ligands and is consequently less reactive, resulting in slow epitaxial growth. The epitaxial growth

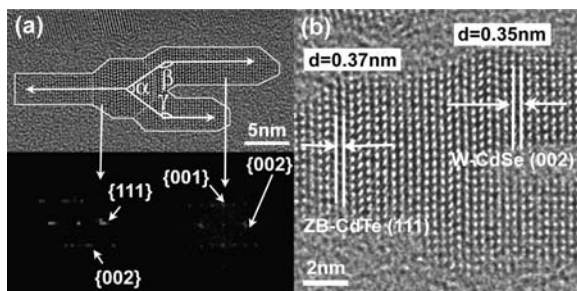


**Figure 2.** HRTEM images of a typical Y-shaped NH: (a) overview image ( $\alpha = 71^\circ$ ,  $\beta = 145^\circ$ ,  $\gamma = 142^\circ$ ) and fast Fourier transforms of corresponding parts; (b) an enlarged picture with lattice distances indicated.

on the  $\text{Te}^{2-}$  ended facet is relatively fast and, thus, produces stacking faults, like those we observe.<sup>6</sup>

Evidence that the colloids are CdTe-CdSe NHs was further obtained by PXRD and energy dispersive spectra (EDS) techniques (see SI Figure S4). The PXRD patterns of CdTe-CdSe NHs correspond well to the hexagonal CdSe phase with relatively narrower and stronger (002) diffraction, indicating the CdSe arm in anisotropic heterostructures grows perpendicular to the (002) phase crystallographic planes. The emergence of Te at the center part in line-scanned EDS spectra further confirmed the formation of CdTe-CdSe NHs.

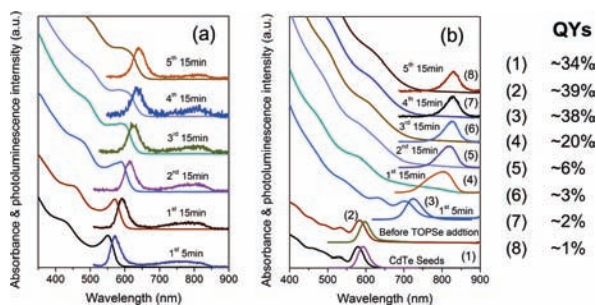


**Figure 3.** Left: Evolution of absorption and PL spectra with the growth of (a) CdSe nanorods and (b) CdTe-CdSe NHs synthesized via epitaxial growth from CdTe seeds with average size of 3.5 nm. Right: PL emission quantum yields (QYs) as a function of NHs epitaxial growth.

Growing CdSe on CdTe is well-known to generate type-II NHs, so that after photoexcitation the hole is confined to CdTe and the electron is located in CdSe. The radiative recombination of the separated electron and hole yields indirect band emission in the near-infrared region, well-shifted from excitonic photoluminescence (PL) of CdTe or CdSe nanocrystals.<sup>4,8</sup> The formation of CdTe-CdSe NHs can thereby be monitored using UV-vis absorption and PL emission spectra. Figure 3 shows the evolution of these spectra during synthesis of CdSe nanocrystals and CdTe-CdSe NHs using 3.5 nm seeds. The spectra of pure CdSe nanocrystals show typical excitonic absorption features and band edge emission together with a broad surface trap state emission, which shift together to a longer wavelength.<sup>23</sup> In comparison, the growth of CdTe-CdSe NHs show an obviously different evolution (Figure 3b; also see SI Figure S5). Taking the epitaxial growth on 3.5 nm seeds for example, the 3.5 nm seeds have a first exciton absorption peak at 580 nm and emission peak at 594 nm. After reaction for 5 min, the absorption of the nanocrystals red-shifted to 720 nm, which suggests the transition to type-II band alignment. Further epitaxial growth leads to the broadening of the first exciton absorption peak,

development of a low-energy tail assigned to interfacial charge transfer state absorption,<sup>24</sup> and emergence of a dominant CdSe absorption feature. During epitaxial growth, only the PL emission in the 700–850 nm region was observed. The PL quantum yields were measured to be ~30–40% for CdTe seeds and during the first 5 min of heterostructure growth. They decreased to ~20% after 15 min and further decreased to ~1% for the final NHs.

In summary, CdTe-CdSe NHs with shapes of rods, fat rods, Y-shape rods, and tetrapods were synthesized simply by using CdTe seeds with different sizes. The tailoring of the shape of nanocrystal heterostructures provides a way to modify charge-transfer and radiative recombination in the near-infrared region. In particular, this advance sets the scene for studying shape-dependent charge-transfer reactions in nanoscale systems where phenomena such as quantum interference might be found.

**Acknowledgment.** The Natural Sciences and Engineering Research Council of Canada is gratefully acknowledged for support of this research. G.D.S. acknowledges the support of an EWR Steacie Memorial Fellowship. The authors thank N. Coombs and S. Petrov for assistance with STEM and XRD measurements, T. Mirkovic, J. He, and J. Tang for discussions.

**Supporting Information Available:** Experimental details, characterization of CdTe seeds, overview STEM images, absorption and PL spectra, X-ray diffraction patterns, energy dispersive X-ray spectra, complete ref 15. This material is available free of charge via the Internet at <http://pubs.acs.org>.

## References

- (1) Scholes, G. D. *Adv. Funct. Mater.* **2008**, *18*, 1157–1172.
- (2) Reiss, P.; Protiere, M.; Li, L. *Small* **2009**, *5*, 154–168.
- (3) Klimov, V. I.; Ivanov, S. A.; Nanada, J.; Achermann, M.; Bezel, I.; McGuire, J. A.; Piryatinski, A. *Nature* **2007**, *447*, 441–446.
- (4) Kim, S.; Fisher, B.; Eisler, H. J.; Bawendi, M. G. *J. Am. Chem. Soc.* **2003**, *125*, 11466–11467.
- (5) Ivanov, S. A.; Piryatinski, A.; Nanada, J.; Tretyak, S.; Zavadil, K. R.; Wallace, W. O.; Werder, D.; Klimov, V. I. *J. Am. Chem. Soc.* **2007**, *129*, 11708–11719.
- (6) Smith, A. M.; Mohs, A. M.; Nie, S. M. *Nat. Nanotechnol.* **2009**, *4*, 56–63.
- (7) Milliron, D. J.; Hughes, S. M.; Cui, Y.; Manna, L.; Li, J. B.; Wang, L. W.; Alivisatos, A. P. *Nature* **2004**, *430*, 190–195.
- (8) Kumar, S.; Jones, M.; Lo, S. S.; Scholes, G. D. *Small* **2007**, *3*, 1633–1639.
- (9) He, J.; Lo, S. S.; Kim, J. H.; Scholes, G. D. *Nano Lett.* **2008**, *8*, 4007–4013.
- (10) Shieh, F.; Saunderson, A. E.; Korgel, B. A. *J. Phys. Chem. B* **2005**, *109*, 8538–8542.
- (11) Halpert, J. E.; Porter, V. J.; Zimmer, J. P.; Bawendi, M. G. *J. Am. Chem. Soc.* **2006**, *128*, 12590–12591.
- (12) Xie, R. G.; Kolb, U.; Basche, T. *Small* **2006**, *2*, 1454–1457.
- (13) Zhong, H. Z.; Zhou, Y.; Yang, Y.; Yang, C. H.; Li, Y. F. *J. Phys. Chem. C* **2007**, *111*, 6538–6543.
- (14) Habas, S. E.; Lee, H. J.; Radmilovic, V.; Somorjai, G. A.; Yang, P. D. *Nat. Mater.* **2007**, *6*, 692–697.
- (15) Carbone, L.; et al. *Nano Lett.* **2007**, 2942–2950.
- (16) Talapin, D. V.; Nelson, J. H.; Shevchenko, E. V.; Aloni, S.; Sadtler, B.; Alivisatos, A. P. *Nano Lett.* **2007**, *7*, 2951–2959.
- (17) Han, W.; Yi, L. X.; Zhao, N.; Tang, A. W.; Gao, M. Y.; Tang, Z. Y. *J. Am. Chem. Soc.* **2008**, *130*, 13152–13161.
- (18) Dorfs, D.; Salant, A.; Popov, I.; Banin, U. *Small* **2008**, 1319–1323.
- (19) Hewa-Kasakarage, N. N.; Kirsanova, M.; Nemchinov, A.; Schmall, N.; El-Khoury, P. Z.; Tarnovsky, A. N.; Zamkov, M. *J. Am. Chem. Soc.* **2009**, *131*, 1328–1334.
- (20) Fiore, A.; Matria, R.; Lupo, M. G.; Lanzani, G.; Giannini, C.; Carlino, E.; Morello, G.; De Giorgi, M. D.; Li, Y. Q.; Cingolani, R.; Manna, L. *J. Am. Chem. Soc.* **2009**, *131*, 2274–2282.
- (21) Yu, W. W.; Wang, Y. A.; Peng, X. G. *Chem. Mater.* **2003**, *15*, 4300–4308.
- (22) Manna, L.; Scher, E. C.; Alivisatos, A. P. *J. Am. Chem. Soc.* **2000**, *122*, 12700–12706.
- (23) Peng, Z. A.; Peng, X. G. *J. Am. Chem. Soc.* **2002**, *124*, 3343–3353.
- (24) Scholes, G. D.; Jones, M.; Kumar, S. *J. Phys. Chem. C* **2007**, *111*, 13777–13785.

JA903722D